


RNAi Screening Reveals Proteasome- and Cullin3- Dependent Stages in Vaccinia Virus Infection

Journal Article**Author(s):**

Mercer, Jason; [Snijder, Berend](#) ; Sacher, Raphael; Burkard, Christine; Bleck, Christopher Karl Ernst; Stahlberg, Henning; Pelkmans, Lucas; Helenius, Ari

Publication date:

2012-10

Permanent link:

<https://doi.org/10.3929/ethz-b-000061389>

Rights / license:

[Creative Commons Attribution-NonCommercial-NoDerivs 3.0 Unported](#)

Originally published in:

Cell Reports 2(4), <https://doi.org/10.1016/j.celrep.2012.09.003>

RNAi Screening Reveals Proteasome- and Cullin3-Dependent Stages in Vaccinia Virus Infection

Jason Mercer,^{1,5} Berend Snijder,^{3,5} Raphael Sacher,² Christine Burkard,¹ Christopher Karl Ernst Bleck,⁴ Henning Stahlberg,⁴ Lucas Pelkmans,^{3,*} and Ari Helenius^{1,*}

¹Institute of Biochemistry

²Institute of Molecular Systems Biology
ETH Zürich, 8093 Zürich, Switzerland

³Institute of Molecular Life Sciences, University of Zürich, 8057 Zürich, Switzerland

⁴Center for Cellular Imaging and NanoAnalytics (C-CINA), Structural Biology and Biophysics, University Basel, Biozentrum, 4058 Basel, Switzerland

⁵These authors contributed equally to this work

*Correspondence: lucas.pelkmans@imls.uzh.ch (L.P.), ari.helenius@bc.biol.ethz.ch (A.H.)

<http://dx.doi.org/10.1016/j.celrep.2012.09.003>

SUMMARY

A two-step, automated, high-throughput RNAi silencing screen was used to identify host cell factors required during vaccinia virus infection. Validation and analysis of clustered hits revealed previously unknown processes during virus entry, including a mechanism for genome uncoating. Viral core proteins were found to be already ubiquitinated during virus assembly. After entering the cytosol of an uninfected cell, the viral DNA was released from the core through the activity of the cell's proteasomes. Next, a Cullin3-based ubiquitin ligase mediated a further round of ubiquitination and proteasome action. This was needed in order to initiate viral DNA replication. The results accentuate the value of large-scale RNAi screens in providing directions for detailed cell biological investigation of complex pathways. The list of cell functions required during poxvirus infection will, moreover, provide a resource for future virus-host cell interaction studies and for the discovery of antivirals.

INTRODUCTION

Poxviruses are enveloped DNA viruses characterized by their large size, intricate structure, and a complex cytoplasmic replication cycle (Moss et al., 2007). Vaccinia virus (VACV), the prototypic poxvirus used in this study, served as a vaccine during the eradication of smallpox, one of the most devastating diseases of the 20th century (Moss et al., 2007). The potential deployment of the smallpox virus as a biological weapon, risks associated with resumed vaccination, and recent monkeypox outbreaks warrant continued research toward new antipoxvirus agents (Di Giulio and Eckburg, 2004; Harrison et al., 2004).

The VACV lifecycle begins with macropinocytic internalization of the virus into host cells (Huang et al., 2008; Mercer and Helenius, 2008). This is followed by low pH-dependent membrane fusion to release the viral core into the cytosol (Townsend et al., 2006). Postpenetration steps include loss of core-associated lateral bodies, core expansion, and transcription of early viral genes within the expanded core (Dales, 1963; Kates and Beeson, 1970; Moss, 1990; Pedersen et al., 2000). Early messenger RNAs (mRNAs) generate about 100 different viral proteins, including unidentified factors required for DNA uncoating (Joklik, 1964b; Magee and Miller, 1968). During the subsequent uncoating process, cores disappear as visible structures, the viral DNA is released and replicated, intermediate and late genes are expressed, and cytosolic virus factories are formed. While many of the cellular factors and functions required for initial entry have been described (Huang et al., 2008; Laliberte et al., 2011; Mercer and Helenius, 2008; Schmidt et al., 2012; Townsend et al., 2006), the cellular factors that participate in viral genome uncoating remain largely undefined.

In the last few years, large-scale RNAi screening has become a powerful tool for the analysis of pathogen-host interactions. This approach has been previously applied to a variety of pathogens (reviewed in Cherry, 2009). For VACV, a *Drosophila* kinome screen was used to identify and describe a role for AMP-activated protein kinase (AMPK) during infection (Moser et al., 2010).

Our goal was to elucidate the host factors in human tissue culture cells needed in the VACV life cycle. Using a large-scale RNAi screen, we identified critical cellular processes that the virus exploits during infection. By focusing our validation studies on protein clusters involved in ubiquitin-mediated proteasome degradation, which has been previously implicated in poxvirus DNA replication (Satheshkumar et al., 2009; Teale et al., 2009), we uncovered additional roles for proteasomes and ubiquitination in virus assembly and genome uncoating. In addition, we identified a Cullin3-based ubiquitin ligase, as required for VACV genome replication. Ultimately, this information could facilitate the development of novel antiviral agents that would target the host rather than the virus directly.

RESULTS

RNAi Screening Identifies 188 Cellular Factors Required for VACV Infection

We used an automated, high-content, high-throughput RNAi screen in human tissue culture cells (HeLa) to identify host cell factors and processes required during the VACV life cycle. Using the mature virion (MV) form of a recombinant VACV that expresses enhanced green fluorescent protein (EGFP) under a synthetic early/late viral promoter (VACV-EGFP) (Mercer and Helenius, 2008), we could readily distinguish infected from noninfected cells based on EGFP expression 8 hr postinfection (hpi). Automated fluorescence microscopy and image analysis was employed to score for cell factors required during the replication cycle, up to and including translation of late viral genes, without distinguishing between early and late defects.

To avoid some of the pitfalls encountered in previous virus infection screens (Cherry, 2009; Mohr et al., 2010), we chose to screen a set of 7,000 genes selected for their potential to be inhibited by small compounds (the 7,000 druggable genome library; QIAGEN). Although covering only one-third of human genes, these represent a well-studied and well-annotated cross-section of the full genome, and for these factors, inhibitors and other reagents are more readily available for follow-up studies. In addition, we improved image analysis, hit visualization, and hit validation (Extended Experimental Procedures; Figure S1; Bray et al., 2012; Snijder et al., 2012).

To increase reliability, we introduced a fully automated computational pipeline for high-content image analysis (Carpenter et al., 2006; Snijder et al., 2009). Over 200 quantitative features were extracted from each of 624 million individual cells from 1.45 million images (Carpenter et al., 2006). Using these features as a basis, several iterations of supervised machine learning were applied to identify virus infection, mitosis, apoptosis, and technical phenotypes (Rämö et al., 2009; Snijder et al., 2009) (see Extended Experimental Procedures for details). Cell number and density (population-context) effects were normalized to improve both reproducibility of screening results in different cell lines and consistency of phenotypes obtained by different small interfering RNAs (siRNAs) targeting the same gene (Snijder et al., 2012).

The RNAi screen was carried out in two steps, as detailed in Figure 1A and in experimental procedures. Three nonoverlapping siRNAs against each gene were used in a primary screen and three additional siRNAs in a secondary follow-up screen. Both screens were repeated independently three times. The primary screen using the 7,000 druggable genomes led to the identification of 276 genes, in which two or three of the three siRNAs reduced VACV infection relative to controls (i.e., for the majority, the median over the triplicates of at least two siRNAs had a median absolute deviation less than -1.5 over the whole screen). To provide a resource for future studies of poxvirus–host cell interaction, the full set of images and analysis results have been made available (see Web Resources).

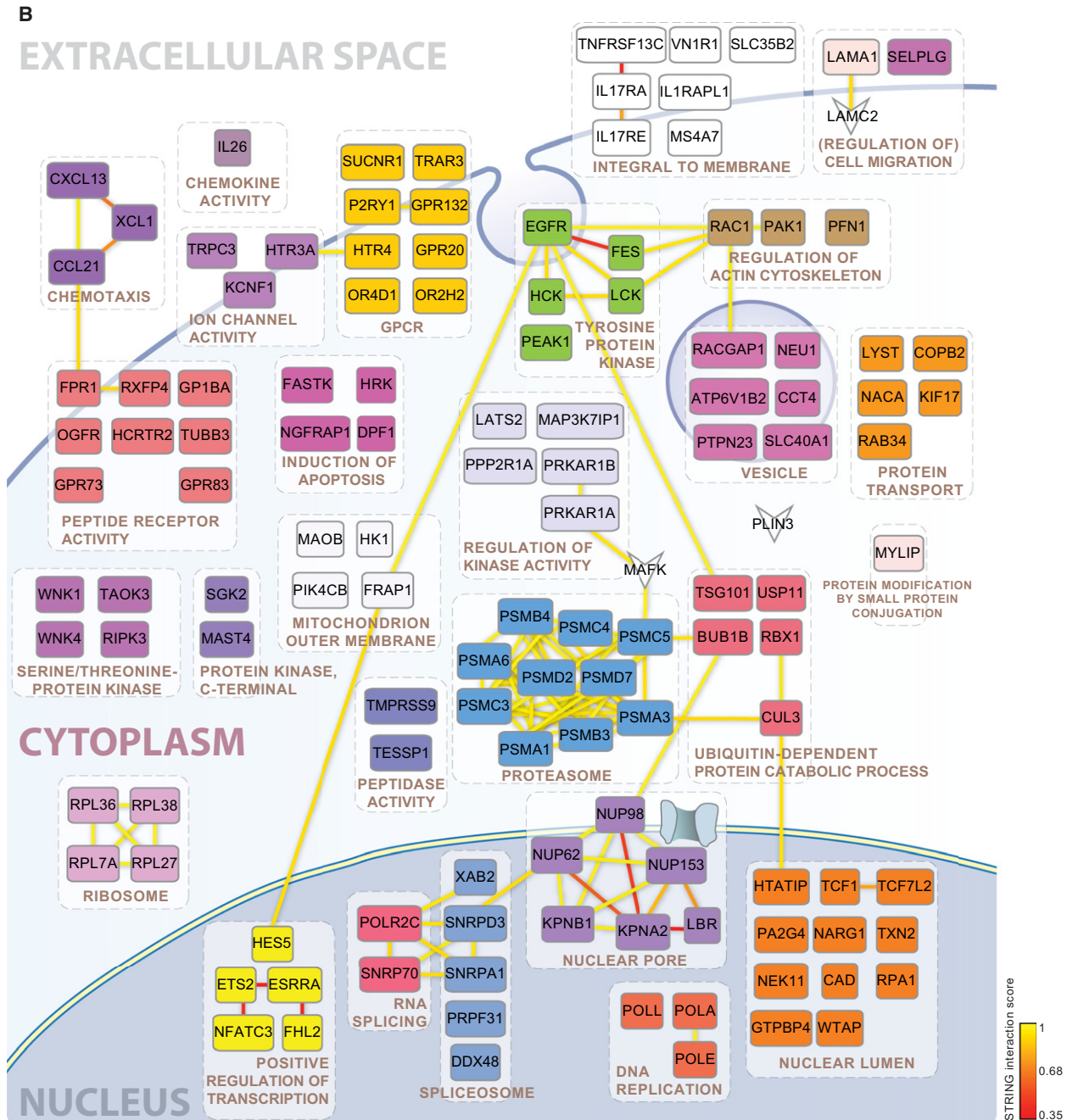
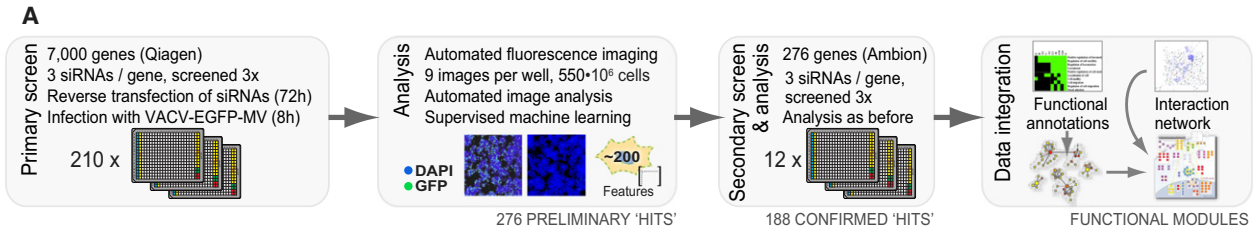
The secondary screen directed against the genes identified as hits in the primary screen was performed using siRNAs from a different vendor (Ambion). It confirmed 68% of the hits from

the primary screen with a correlation coefficient of 0.34 between the validated RNAi phenotypes of the two screens ($p = 2.8 \times 10^{-6}$). A stringent, control-based analysis of nontargeting control siRNAs gave a false positive rate of 0.06% in the secondary screen, giving further confidence in the confirmed host factors.

The final hit list shown in Table S1 had 188 genes, representing a broad range of cell functions. Among them, several proteins have been previously implicated in VACV infection: EGFR, RAC1, PAK1, laminin (LAMA1 and 2), the proteasome, Tsg101, profilin, and RIPK3 (Chiu et al., 2007; Cho et al., 2009; Eppstein et al., 1985; Honeychurch et al., 2007; Li et al., 2008; Locker et al., 2000; Mercer and Helenius, 2008; Mercer et al., 2010; Satheshkumar et al., 2009; Teale et al., 2009; Villa et al., 2010). In the only other high-throughput RNAi screen directed against VACV, Moser et al. screened 440 unique *Drosophila* genes and identified seven hits, of which the human orthologs are PRKAA2, PRKAG2, PRKAB1, PIKfyve, PIK3C2A, STAM, and PTPN23 (Moser et al., 2010). Of these, we identified PRKAB1 and PTPN23 (Figure 1B; Table S1). While no exact match for PIK3C2A was found, PI4KB and FRAP1 were hits, further highlighting the importance of phosphoinositide-kinase activity for VACV infection (McNulty et al., 2010; Mercer and Helenius, 2008; Moser et al., 2010). Other hits, such as ribosomal proteins, were expected for any virus. However, the majority of hits had no prior connection to VACV infection.

To extract information regarding critical processes in the infection cycle, the list was submitted to rigorous bioinformatic analysis. For this, we developed an algorithm that combined functional- and interaction-based information. This algorithm has been made available (see Supplemental Network Visualization Algorithm) and is applicable for the visualization and analysis of any gene list. The hits were first assigned to “functional annotation clusters,” representing sets of proteins that share common annotations within public databases [DAVID; (Huang et al., 2009)]. As shown in Table S2 and Figure S2, the genes were enriched within 13 clusters and several highly connected functional annotation networks.

The function-based information was combined with data on protein interactions between individual host factors (STRING; Szklarczyk et al., 2011). The result of the combined analysis is shown for 126 of the 188 host factors in Figure 1B. Automatic annotation was used to visualize the interaction networks (yellow to red lines) both within and between functional annotation clusters (gray dashed boxes). Without going into detail, it was evident that, although replication and assembly of progeny virus occurs in the cytoplasm of host cells, VACV depends on cytoplasmic as well as nuclear factors. Since the nucleus and its many functions, such as splicing and nuclear pore complex function, have been largely ignored with regard to the infectious lifecycle of poxviruses, these findings are likely to open new avenues in VACV research. The cytoplasmic functions included membrane trafficking, signaling, proteolysis, and ion transport. Factors in the tyrosine kinase and actin clusters have already been shown to be necessary for phosphatidylserine-mediated macropinocytosis of the virus during entry (Mercer and Helenius, 2008; Mercer et al., 2010).



VACV Core Breakdown Requires Proteasome Activity, but Is Independent of New Ubiquitination

In the follow-up, we focused on two prominent clusters: the proteasome and ubiquitination (Figure 1B). Both have been previously implicated in VACV genome replication (Satheshkumar et al., 2009; Teale et al., 2009). siRNA-mediated depletion of proteasome subunits caused a nearly complete block in late viral gene expression (Figure 2A). For confirmation, we determined the virus yield in the presence of MG132, a proteasome inhibitor, and UBEI-41, an inhibitor of the cellular E1 ubiquitin-conjugating enzyme UBA1. Both decreased viral yield by ~3 logs, similar to cycloheximide (CHX), a protein synthesis inhibitor (Figure 2B). When infection with VACV strains that express EGFP specifically from an early (E-EGFP-VACV) or a late (L-EGFP-VACV) promoter was analyzed by flow cytometry, we found that the inhibitors blocked late but not early viral gene expression (Figure 2C).

This suggested that early steps in the virus lifecycle, such as virus binding and endocytosis, were not impacted by these inhibitors. To confirm this, we tested whether the effects of MG132 and UBEI-41 could be circumvented by forcing fusion of virions at the plasma membrane with low pH. This treatment results in deposition of viral cores into the cytoplasm, effectively bypassing the need for endocytosis (Mercer and Helenius, 2008). Consistent with a postpenetration block, the inhibitors could not be bypassed upon low pH treatment (Figure 2D). Viral yield, late gene expression, and inhibition after bypass were also affected when using the more specific proteasome inhibitor, Velcade (Figure S3). Thus, as reported by Teale et al. and Satheshkumar et al. (Satheshkumar et al., 2009; Teale et al., 2009), we found that proteasomes and UBA1 had no role in virus endocytosis and penetration.

Next, we addressed genome uncoating. The efficient release of viral DNA from internalized cores is of interest because poxvirus particles and cores are extremely stable when exposed to desiccation, denaturants, proteases, extremes of temperature, etc. (Essbauer et al., 2007; MacCallum and McDonald, 1957; Malkin et al., 2003).

Using a microscopy-based core stabilization assay that relied on immunofluorescence staining of released cores, Satheshkumar and coworkers reported that inhibition of proteasome activity had only a minor impact on genome uncoating (Satheshkumar et al., 2009). Although over a 2-fold increase in core stabilization was observed in the presence of MG132, they concluded that inhibition of proteasome activity may delay or reduce uncoating, but the effect was not sufficient to account for the reduction in infectivity.

In light of these previous findings and the observation that VACV cores are rapidly and efficiently disassembled during entry into a new host cell (Joklik, 1964b; Magee and Miller, 1968), we found it conceivable that proteasome-directed core

degradation was directly connected to DNA release. To further investigate this possibility, we followed the fate of individual viruses and cores by fluorescence microscopy using a virus in which the core protein A5 was tagged with EGFP (Mercer and Helenius, 2008) and by immunofluorescence staining of the viral membrane protein L1 (Schmidt et al., 2011). HeLa cells were incubated at a multiplicity of infection (MOI) of 10 for 4 hr, a time sufficient for virions to enter and undergo genome uncoating. Intact virions that still contained the viral membrane were yellow (closed arrowheads), and internalized, released viral cores devoid of membrane were green (open arrowheads). When the cores in control cells were quantified (Figure S4), few were observed (25–50/cell; green) (Figure 2E; untreated [UNTR]). However, in the presence of CHX, which prevents core breakdown and genome uncoating (Joklik, 1964b), intact cytoplasmic cores numbered 275–320 per cell (Figure 2E; CHX). The same was observed when the proteasome was inhibited with MG132 (250–300/cell) (Figure 2E; MG132). UBEI-41 had virtually no impact on core breakdown (50–60 cores/cell) (Figure 2E; UBEI-41). This suggested that protein synthesis and the proteasome were needed for uncoating, but UBA1 was not.

When the state of cytoplasmic cores after entry in the presence of MG132 was investigated using electron microscopy, we could confirm that viral cores remained intact (Figure 2F, MG132; Figure S5). While core expansion occurred (Figure S6), it was evident that the genome (i.e., the electron dense material within the cores) was not released (Figure 2F; blow-up). Electron microscopy also showed that, while UBEI-41 did not inhibit core breakdown, it prevented formation of viral DNA replication factories (Figure 2F; UBEI-41). This was consistent with previous reports that ubiquitination is needed for DNA replication (Satheshkumar et al., 2009; Teale et al., 2009). Taken together, the results suggested, somewhat paradoxically, that proteasomes were needed for breakdown of the core, whereas ubiquitination, which normally serves to prepare substrates for degradation, was required for a subsequent step, one preceding DNA replication.

The microscopy-based uncoating assays used by Satheshkumar and coworkers and here by us rely on core destabilization as an indicator of genome uncoating. However, the release of parental genomes from incoming viral cores is not analyzed. Thus, it was possible that the viral DNA was released from viral cores in the presence of MG132, but the cores themselves were not degraded in the absence of proteasome activity. To directly monitor release of incoming viral DNA as a consequence of core breakdown, we used immunofluorescence staining for the viral protein I3L that is bound to the viral DNA (Welsch et al., 2003). That antibodies directed against this protein can be used to detect uncoated parental VACV DNA in the absence

Figure 1. VACV RNAi Screen and Functional Map of Host Factors Required for Infection

(A) Outline of screening and bioinformatic procedures.

(B) Host factors in larger functional clusters that interact or share functional annotations are depicted. Individual genes were assigned to the highest enriched functional annotation cluster in which they were present (Figure S2). Functional clusters identified by DAVID with simplified annotations (Table S2) are pictured as white boxes with dashed outlines. Yellow lines between genes of different clusters indicate high-confidence (>0.9) STRING interactions, while those between genes within the same functional cluster include lower confidence (>0.35) STRING interactions. Selected genes not found within a functional annotation cluster are indicated as inverted arrowheads. Functional gene clusters are pictured in their approximate cellular location.

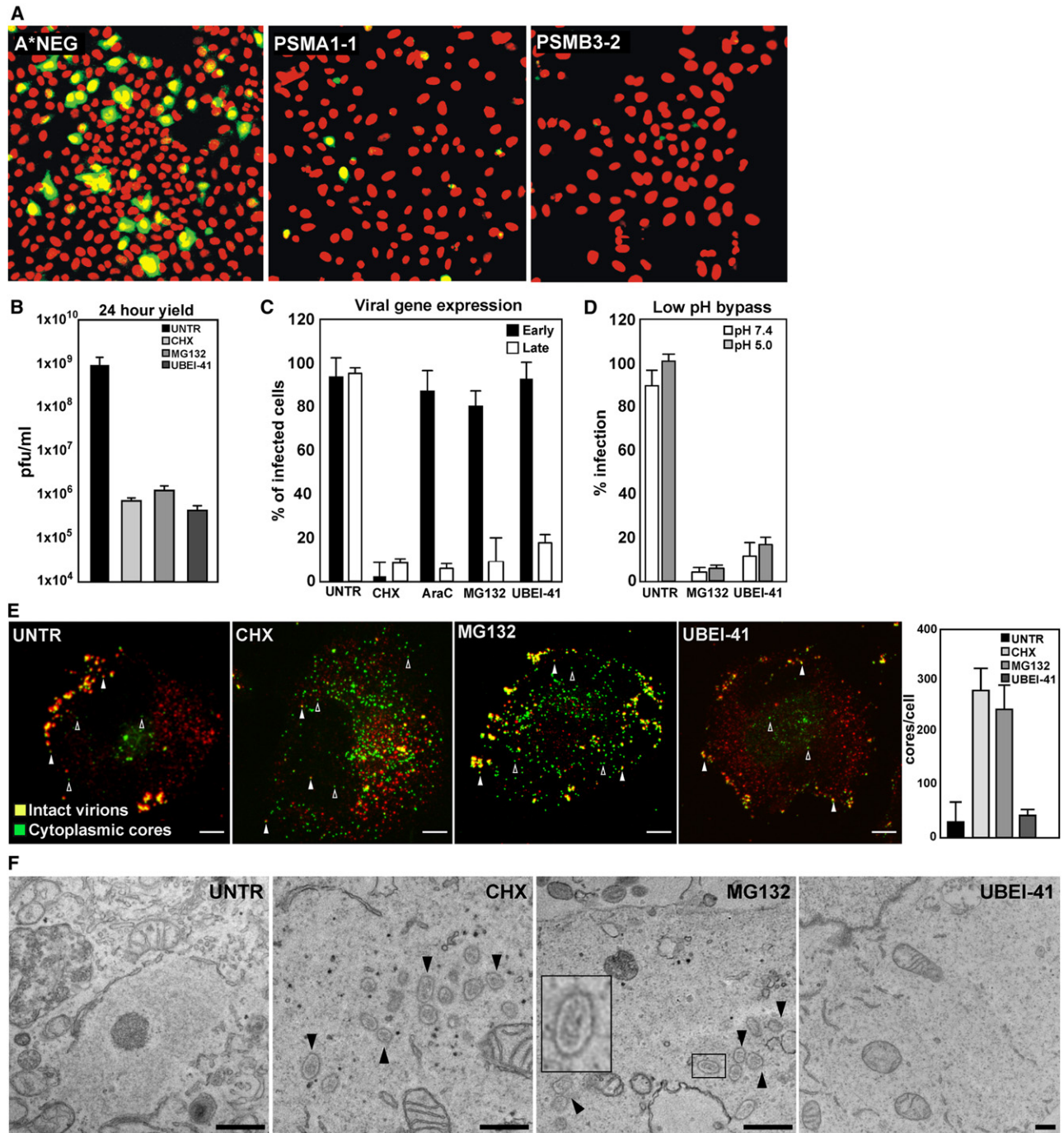


Figure 2. Proteasome but not E1-Activating Enzyme Function Is Required for VACV Genome Uncoating

(A) RNAi-mediated silencing of proteasome subunits PSMA1 and PSMB3 impair VACV infection. Representative images from the screen are displayed with nuclei in red and infected cells in green.

(B) Proteasome (MG132) and E1-activating enzyme (UBEI-41) inhibitors block VACV production (MOI 1; 24 hpi; 10 μ M AraC, 10 μ g/ml CHX, 25 μ M MG132, and 50 μ M UBEI-41 used throughout).

(C) MG132 and UBEI-41 allow for early but not late VACV gene expression. Cells were infected with VACV (MOI 1), expressing EGFP from either an early (Early) or a late (Late) promoter. Infections were performed in the presence of the indicated inhibitors. Cells were harvested 6 hpi and analyzed for the number of early or late EGFP-expressing cells, respectively. Cells infected in the presence of CHX or AraC were used as controls.

(D) MG132 and UBEI-41 inhibit VACV infection after internalization. VACV-EGFP MVs (MOI 1) were bound to cells for 1 hr in the presence of inhibitors. Cells were then washed, treated with pH 7.4 or pH 5.0 media for 5 min, washed, and media containing the inhibitors added back. Cells were analyzed by flow cytometry for EGFP at 6 hpi.

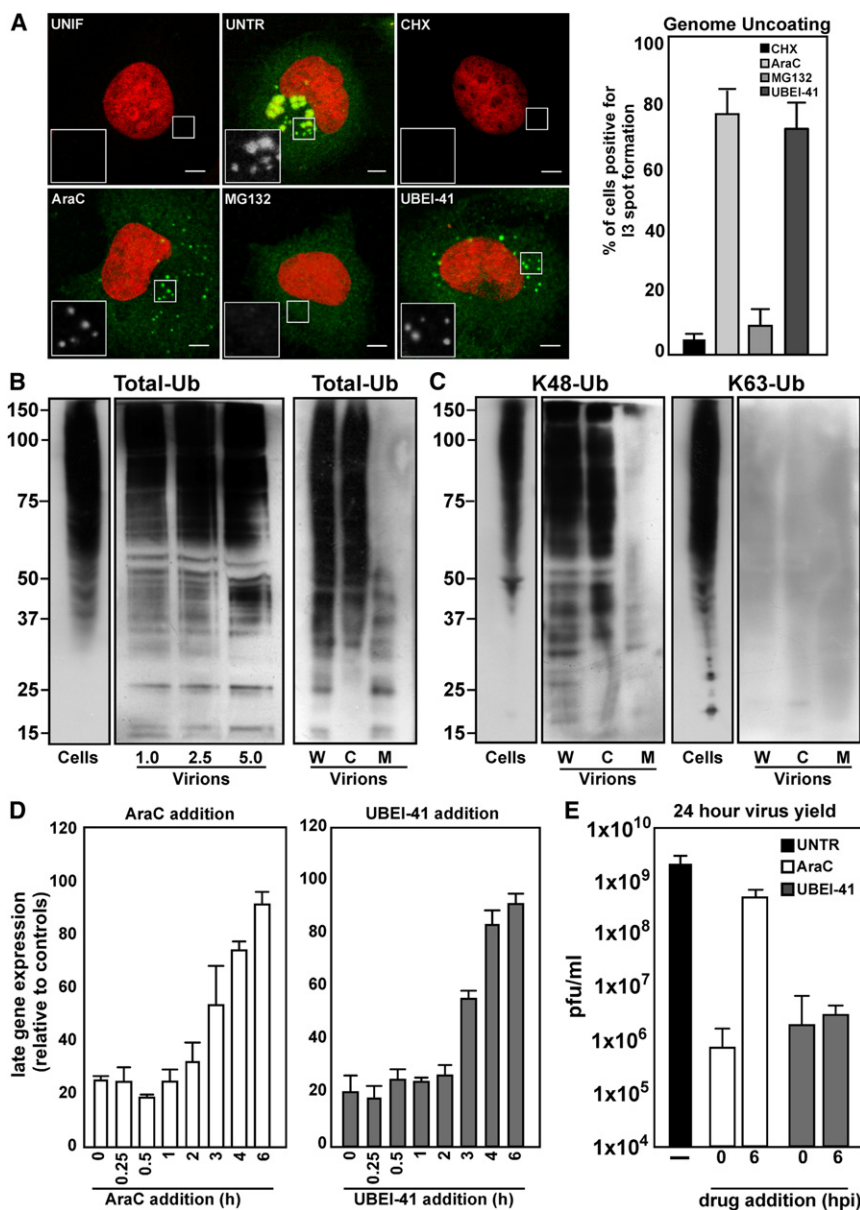


Figure 3. Polyubiquitination of VACV Cores Facilitates Their Degradation and Subsequent Genome Uncoating

(A) MG132 prevents VACV genome release, and UBEI-41 blocks viral DNA replication. Cells were infected (MOI 10) in the absence of inhibitors (UNTR) or in the presence of MG132 or UBEI-41. Cells were fixed at 4 hpi and immunofluorescence against the viral DNA binding protein, I3, performed, followed by staining of nuclei with Dra5. In all images, nuclei are colored red and I3 staining is in green. Cells treated with CHX, which prevents genome release, or AraC, which allows for release of parental genomes, but not their replication, served as controls for the assay. Scale bars, 10 μ m. The number of cells positive for parental DNA staining (I3 spot formation) under each condition is displayed as the mean \pm SD (right). (B) VACV core proteins are packaged in a polyubiquitinated state. Immunoblots directed against total (mono and poly) ubiquitin were performed on 1.0, 2.5, and 5.0 μ g of purified VACV MVs (left), on 2.5 μ g of whole (W) VACV MVs, or MVs separated into core (C) and membrane (M) fractions (right). As a control for the detection of ubiquitin, 100 μ g of cell lysate (Cells) was used. Experiments were performed in triplicate and representative blots shown.

(C) Viral core proteins are positive for K48-, but not K63-linked ubiquitin chains. Immunoblots directed against K48- or K63-specific ubiquitin chains were performed on whole (W), core (C), and membrane (M) fractions of VACV MVs. One hundred micrograms of cell lysate was used as a control for each antibody (Cells).

(D) Late addition of MG132 or UBEI-41 does not impede late viral gene expression. Cells were infected (MOI 1) with VACV-EGFP-LATE. Either 10 μ M AraC or 50 μ M UBEI-41 were added at the indicated times. Infection was allowed to proceed for a total of 12 hr before cells were harvested and analyzed by flow cytometry for EGFP expression. Values are displayed as the percentage of cells expressing late genes relative to untreated infected control cells at 12 hpi.

(E) Inhibition of E1-ligase function at 6 hpi impedes production of infectious virus. Cells were infected with VACV MVs (MOI 1) and AraC or UBEI-41 added at either the time of infection (0) or after 6 hr (6). Cells were harvested 24 hpi, and the

progeny virus was purified by banding (Figure S8), followed by titration for plaque-forming units/ml. (A)–(C) Experiments were performed in triplicate and representative images shown. (D) and (E) Experiments were performed in triplicate and displayed as the mean \pm SD.

See also Figures S7 and S8.

of viral replication has been demonstrated (Domi and Beaud, 2000; Welsch et al., 2003). While unable to access the antigen in intact cores (Figure S7), antibodies to I3L stained cytoplasmic

viral DNA after release from incoming cores (Figure 3A). Later in infection, it also stained the I3L complexed with viral DNA in the large perinuclear virus factories. When control cells were

(E) VACV core degradation is proteasome-, but not E1-activating enzyme-dependent. Cells were infected with WR-EGFP-A5 (MOI 10) in the presence of CHX, MG132, or UBEI-41. At 4 hpi, cells were fixed and intact virions identified by immunofluorescence against the viral membrane protein L1R. Representative yellow intact virions are marked by closed arrowheads and free green cytoplasmic cores by open arrowheads. Experiments were performed in triplicate, and the average number of cores per cell under each condition displayed as mean \pm SEM (right) (Figure S4). Scale bars, 10 μ m.

(F) Electron microscopy (EM) shows that MG132 and UBEI-41 inhibit distinct stages of the VACV lifecycle. Cells treated as in (F) (MOI 10; 4 hpi) were analyzed by EM. Intact viral cores are indicated by arrowheads. Blowup of virion (MG132) indicates that the electron dense viral genome is still within the core. Scale bars, 500 nm. All experiments have been performed in triplicate and displayed as the mean \pm SD (B)–(D) or representative images displayed (A), (E), and (F).

See also Figures S3, S4, S5, and S6.

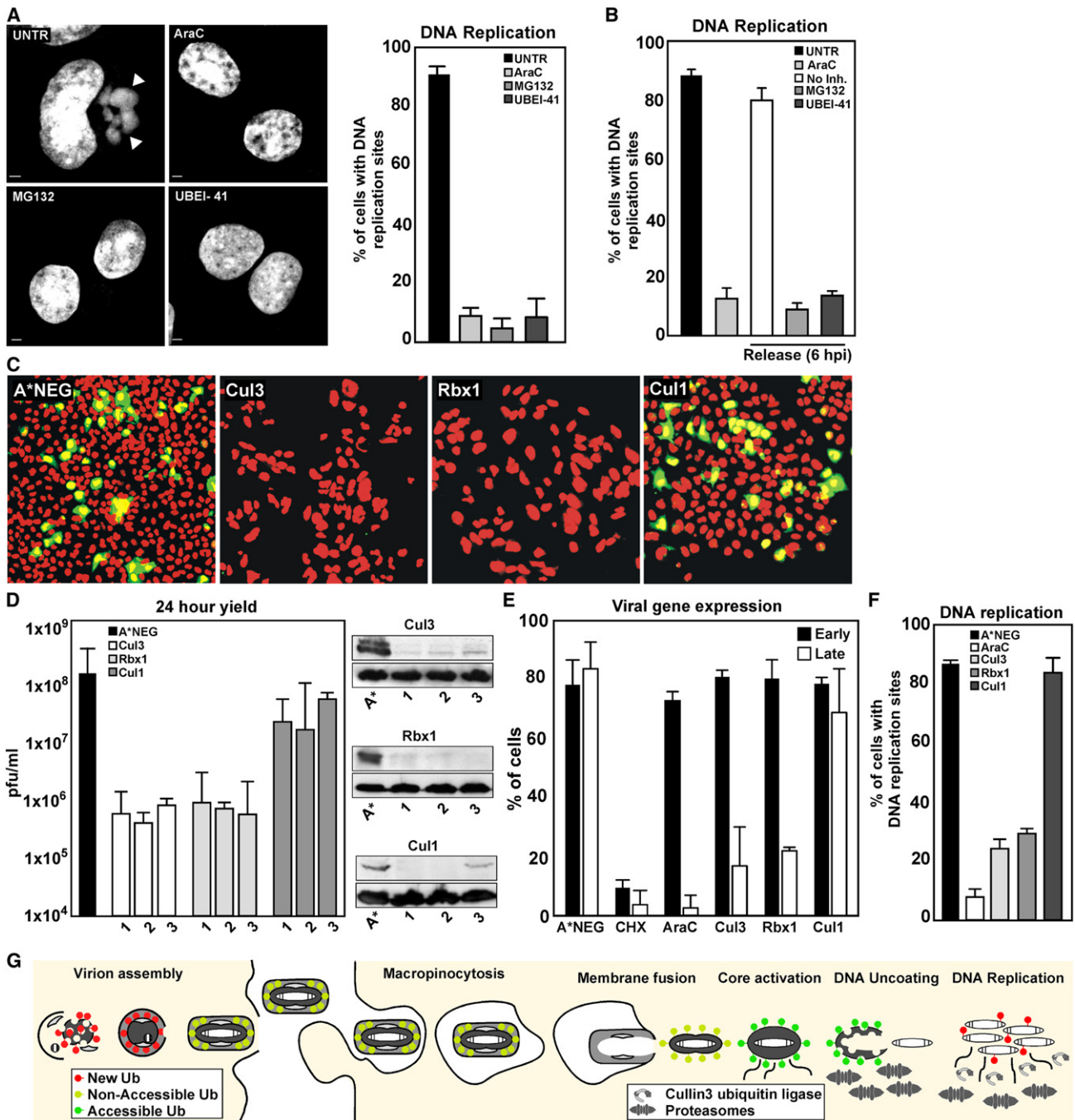


Figure 4. A Cullin3 E3-Ligase Complex Is Required for VACV DNA Replication

(A) MG132 and UBEI-41 block VACV DNA replication site formation. Cells were infected with VACV MVs (MOI 1) in the presence of AraC, MG132, or UBEI-41. Cells were fixed and stained for DNA at 4 hpi. Representative images (left) scale bars, 2 μ m; mean \pm SD of triplicate experiments (right).

(B) MG132 and UBEI-41 block VACV DNA replication after uncoating. Cells were infected with VACV MVs (MOI 1) in the presence of AraC. At 6 hpi, cells were washed and released from AraC (No Inh.) or shifted into MG132 or UBEI-41. Cells were fixed at 12 hpi and assessed for the presence of cytoplasmic DNA replication sites.

(C) RNAi against Cul3 or Rbx1, but not Cul1, impairs VACV infection. Representative images from the screen are displayed with nuclei in red and infected cells in green.

(D) Silencing of Cul3 or Rbx1, but not Cul1, reduces virus production. Cells were reverse transfected with 20 nM (final concentration) of three independent siRNAs directed against either Cul3, Rbx1, or Cul1. After 72 hr, cells were infected with VACV MVs (MOI 1). Twenty-four hours later, cells were harvested and lysates titered for plaque-forming units/ml (left). Immunoblot analysis of Cul3, Rbx1, and Cul1 after siRNA mediated silencing for 72 hr. Immunoblot analysis directed against actin was used as a loading control (right; representative blots shown).

infected for 4 hr at a MOI of 10 and the viral DNA visualized by anti-I3L, replication factories and cytoplasmic I3 staining were seen (green) (Figure 3A; UNTR). With CHX present to prevent early gene expression and genome release, only 5% of cells had I3L-positive spots in the cytoplasm. In the presence of cytosine arabinoside (AraC), an inhibitor of viral DNA replication, 78% of cells contained cytoplasmic I3L spots, indicating that incoming viral DNA had been released, but not replicated. Cells infected in the presence of MG132 were positive for diffuse cytoplasmic I3L staining, but did not contain I3L-positive viral DNA spots. This showed that, even though expression of I3L (an early protein) had occurred, viral genomes had not been released (Figure 3A; MG132). In contrast, UBEI-41-treated cells displayed diffuse cytoplasmic I3L staining and I3L-positive spots, as seen in AraC-treated cells, confirming that viral genomes were released but not replicated. Collectively, these results showed that the proteasome and UBA1 acted in distinct steps in the early infection cycle: proteasomes in core breakdown and DNA release and UBA1 (and thus ubiquitination) in replication of released viral DNA.

VACV Core Proteins Are Packaged in a K48-Ubiquitinated State to Mediate Proteasome-Dependent Genome Uncoating

That core degradation was not dependent on UBA1 suggested that ubiquitin must have been added to core proteins prior to virus entry. Proteomic analysis of isolated VACV virions has indicated that ubiquitin accounts for 1–3 mole percent of total protein (Chung et al., 2006). However, the location of this ubiquitin within the viral particle and the potential role of this host protein in the virus lifecycle have not been investigated.

Immunoblot analysis on highly purified VACV virions confirmed that they contained a striking amount of ubiquitin (Figure 3B, left). The molecular weight of the detected bands indicated that these were ubiquitin-conjugated proteins and not free ubiquitin. To assess the location of the ubiquitin-conjugated proteins, virions were separated into membrane and core fractions (Mercer and Traktman, 2003). Immunoblot analysis on these fractions indicated that the vast majority of the ubiquitinated factors were components of the viral core (Figure 3B, right). Using lysine-48- and lysine-63-linked polyubiquitin specific antibodies, we showed that only lysine-48-linked ubiquitinated proteins were present (Figure 3C). Since lysine-48-linked ubiquitin chains mark proteins for proteasomal degradation (Clague and Urbé, 2010; Komander, 2009), it was evident that this was the mechanism that triggered proteasome-mediated genome uncoating.

Since ubiquitination of core proteins must occur during virion production in infected cells, we asked whether infectious virus could be produced if ubiquitination was inhibited late in infection. Addition of AraC at 6 hr had little effect on late viral gene expression (Figure 3D, white) and only marginally reduced the 24 hr virus yield (Figure 3E, white). As late genes are expressed from newly replicated genomes, this indicated that, by 6 hpi, viral DNA replication and late gene expression was sufficient for significant virus production. When UBEI-41 was added at 6 hpi, again there was no impact on late viral gene expression (Figure 3D, gray). However, unlike AraC, which had little effect on virus yield, addition of UBEI-41 after 6 hr prevented the production of infectious virus (Figure 3E, gray). We were, in fact, unable to isolate virus particles from infected cells treated with UBEI-41 from 6 hpi (Figure S8). This indicated that there are at least two steps in the VACV infectious cycle that require ubiquitination: not only viral DNA replication after genome uncoating, but also assembly of progeny virus.

A Cullin-3 Ubiquitin Ligase Complex Is Required for VACV Genome Replication

It has been reported that poxvirus DNA replication is inhibited in MG132- and Velcade-treated cells (Satheshkumar et al., 2009; Teale et al., 2009). Could this observation be explained by the upstream inhibition of uncoating, or was there a second step in the early infection program that required ubiquitination and the proteasome? After confirming that both MG132 and UBEI-41 prevented VACV replication site formation (Figure 4A), we used an AraC wash-out assay to test for direct effects on replication. AraC has no impact on the uncoating of viral genomes, but prevents their replication. Cells were infected in the presence of AraC for 6 hr to allow uncoating, but to stop replication of incoming genomes. AraC was then washed out or replaced with either UBEI-41 or MG132. Infection was allowed to proceed for an additional 6 hr, after which cells were analyzed for viral replication sites (Figure 4B). In control cells without a second inhibitor (No Inh.), replication site formation was normal. However, in the presence of UBEI-41 or MG132, the formation of viral replication sites did not occur. These results confirmed that the initiation of DNA replication requires both a ubiquitination step and proteasome-mediated degradation.

Reasoning that a cellular ubiquitin ligase was likely to be involved, we turned to the hits in the RNAi screen. The ubiquitin functional annotation cluster (Figure 1B) contained two components of the BCR E3 ubiquitin-ligase complex: Cullin3 (Cul3) and RING-box protein 1 (Rbx1). Images from the screen indicated that depletion of these factors resulted in the absence of

(E) Silencing of Cul3 and Rbx1, but not Cul1, reduces late but not early viral gene expression. Cells were subjected to siRNA-mediated silencing as in (D) followed by infection with VACV (MOI 1), expressing EGFP specifically from an early or a late promoter. Cells were harvested 6 hpi and analyzed for the number of cells expressing early and late EGFP, respectively. Cells infected in the presence of CHX or AraC were used as controls.

(F) Cul3 and Rbx1 are required for VACV DNA replication site formation. Cells in which Cul3, Rbx1, or Cul1 had been silenced (20 nM siRNA; 72 hr) were infected with VACV MVs (MOI 1). At 4 hpi, cells were fixed, stained with DraQ5, and analyzed for the presence of viral DNA replication sites. Experiments were performed in triplicate and displayed as mean \pm SD (A, B, and D–F).

(G) Model of VACV core ubiquitination, core degradation/genome uncoating, and genome replication. During assembly of VACV MVs, viral core proteins are ubiquitinated in a K48-linked fashion. Upon infection of naive cells, fusion of viral and cellular membranes releases the ubiquitinated viral core into the cytoplasm. A first round of cellular proteasome action directs the degradation of the ubiquitinated core and concomitant genome release. A Cul3-based ubiquitin ligase and second round of proteasome action serves to initiate replication of the released viral genomes. Ubiquitination events: new (red); nonaccessible (yellow); accessible (green); proteasomes (gray bullets); cullin-based ubiquitin ligase complex (gray crescents).

late gene expression (Figure 4C). A requirement for Cul3 and Rbx1 was validated with three independent siRNAs each. Depletion of either factor decreased the 24 hr viral yield by two logs (Figure 4D; left). Silencing of Cullin-1 (Cul1), a component of the SCF E3 ubiquitin-ligase complex that was not a hit in the screen, had no impact (Figure 4C and 4D; left). The knockdown efficiency of these siRNAs was confirmed by Western blot (Figure 4D; right).

Additional experiments were performed using the siRNA with the strongest knockdown efficiency (Cul3-1, Rbx1-3, and Cul1-2). Depletion of Cul3 or Rbx1 was found to significantly decrease late but not early gene expression (Figure 4E), mirroring the effect of AraC and confirming a defect in DNA replication. In line with this, Cul3 and Rbx1 knockdown inhibited the formation of cytoplasmic DNA replication factories (Figure 4F). We concluded that UBA1, a Cul3 ubiquitin ligase, and the proteasome were required to initiate the replication of uncoated VACV DNA.

DISCUSSION

Our results demonstrated that large-scale RNAi screening can, despite inherent problems and pitfalls (off-target effects, insufficient knockdown, cell population context effects, incomplete genome annotation, etc. [Cherry, 2009; Mohr et al., 2010]) serve as a valuable tool in the study of pathogen/host interactions. The positive outcome relied in this case on a robust image-based assay, on supervised classification of cellular phenotypes, a separation of indirect and direct effects of siRNAs, and on improved bioinformatics analysis to identify gene clusters (Snijder et al., 2012). That the screening data, analysis, and bioinformatic tools used for the purpose of this study are publicly available will be of general usefulness in the analysis of future screening data.

Among the 188 hits, we identified numerous clusters in which multiple hits occurred in the same pathway or complex. Regarding the validity of the final hit list, we are encouraged by how many of the hits corresponded to factors identified earlier as essential genes in VACV infection. Validation studies with two of the clusters as a starting point allowed us to extend previous findings regarding a role for ubiquitination in DNA replication (Satheshkumar et al., 2009; Teale et al., 2009) and discover a new role for ubiquitination and the proteasome in virus assembly and uncoating (Figure 4G). We could thus confirm the value of the hit list as a resource for functional studies of poxvirus host cell interactions.

Our results showed that ubiquitination comes into play as an essential process already during the assembly of VACV particles in virus factories located in the cytoplasm of producer cells. Core proteins undergo extensive K48-linked polyubiquitination. This is consistent with the accumulation of ubiquitin observed in poxvirus replication sites and the detection of ubiquitin within purified VACV particles (Chung et al., 2006; Nerenberg et al., 2005). Polyubiquitination is probably an essential step in virus assembly, because inhibition of the E1 ubiquitin-activating enzyme prevented the generation of viral particles. VACV encodes one ubiquitin ligase, p28, which localizes to VACV replication sites (Nerenberg et al., 2005). However, as this protein is not required for virus production in tissue culture, it is unlikely to

be the ligase responsible for the ubiquitination of viral core proteins. Future work is needed to identify the core components that are ubiquitinated as well as the ubiquitin ligase(s) responsible. During egress from the viral factory, the viral membrane may protect the ubiquitinated core proteins from the degradation machinery.

After macropinocytic internalization of VACV into a new host cell and low pH-dependent membrane fusion, polyubiquitinated cores are released into the cytosol. They immediately undergo activation marked by major expansion in size, a step that does not require early gene expression (Dales, 1963; Ichihashi et al., 1984; Pedersen et al., 2000). The expanded cores serve as the site for early gene transcription (Joklik, 1964a; Magee and Miller, 1968). That they are not yet substrates for proteasome-mediated uncoating suggests that the ubiquitin chains are not accessible. For degradation of the core and uncoating of the DNA, early genes have to be expressed. One or more of the early proteins are likely responsible for making the ubiquitinated core proteins accessible as substrates for the proteasome. The core particle is destroyed and some of the core components, such as the A5 protein, degraded.

As a result of the proteolysis, the viral DNA genome is released and the core itself is no longer recognizable as a structure in the cytosol. That UBA1 activity is not required indicates that the ubiquitin present in the core is sufficient to mediate genome uncoating. Although proteasome function has been implicated in the regulation of viral trafficking, replication, egress, and immune evasion (reviewed in Banks et al., 2003), a direct role for proteasomes in the uncoating of viruses or viral capsids has not, to our knowledge, been observed before.

It was previously reported that viral DNA replication requires ubiquitination and proteasome activity (Satheshkumar et al., 2009; Teale et al., 2009). Our results extended these findings to show that replication of the viral DNA depends on Cul3 and Rbx1, two components of an important, multifunctional E3-ligase family (Petroski and Deshaies, 2005). As recently reviewed (Barry et al., 2010), VACV encodes at least four Cul3 substrate adaptors: A55R, C2L, C5L, and F3L (Beard et al., 2006; Froggatt et al., 2007; Pires de Miranda et al., 2003). Although each of these is required for VACV virulence, they are not essential for replication in tissue culture. This implies that they are not the adaptor proteins used by Cul3 to facilitate VACV DNA replication. While the substrates are yet to be identified, one possibility is that they represent remaining DNA-associated proteins to be removed before replication.

The proteasome thus plays a central role in at least two steps in the replication cycle of VACV. Collectively, the RNAi screen and follow-up studies, like those described here, are likely to provide a starting point for detailed cell and molecular biology analysis of poxvirus-host cell interactions, and they may facilitate the development of novel antipoxvirus agents that target the host cell rather than viral factors.

EXPERIMENTAL PROCEDURES

RNAi Screen

HeLa MZ cells from Marino Zerial (MPI-CBG, Dresden) were maintained at 37°C and 5% CO₂ in Dulbecco's modified Eagle's medium (DMEM; GIBCO

BRL) supplemented with 10% fetal calf serum (FCS) and glutamax. All liquid-handling steps, including preparing cell plates, virus infection, and cell fixation, were performed on a Freedom Evo200 liquid-handling robot (Tecan) set up specifically for this purpose. Seeding, fixing, and DAPI staining of the cells was performed using a Matrix Wellmate Microplate Dispenser (Thermo Scientific).

RNA interference against the 6,979 gene targets was achieved with three independent siRNAs targeting each (siRNAs #1 and #2 from QIAGEN druggable genome version 2 and siRNA #3 from QIAGEN druggable genome version 3) or three independent siRNAs from Ambion for secondary screening (custom ordered). Each siRNA was tested in triplicate. Experiments were conducted in a 384 well plate format, amounting to 210 plates for the primary screen (see [Extended Experimental Procedures](#) for plate layout).

All images were acquired on automated wide field cellWoRx microscopes (Applied Precision) with a 10X objective, and 2 × 2 binning per pixel. Multiwell plates were loaded onto the cellWoRx microscopes using Freedom Evo robotics from Tecan. Three by three directly adjacent images were taken per well, covering over ~90% of each well surface. An image-based autofocus was performed on the DAPI signal for each imaged site. The images were recorded with 12-bit charge-coupled device (CCD) cameras and stored as individual 16-bit uncompressed tagged image file format (TIFF) files per imaged site and per channel.

Computational Image Analysis, Supervised Classification of Cellular Phenotypes, Hit Scoring, DAVID Annotation Clustering Network, and Combined DAVID/STRING Functional Gene View

Please refer to the [Extended Experimental Procedures](#) for details on bioinformatics methodology.

Cells, Viruses, and Reagents

HeLa ATCC and HeLa MZ cells were maintained at 37°C and 5% CO₂ in DMEM (GIBCO BRL) supplemented with 10% FCS and glutamax. Wild-type vaccinia virus (strain WR), (EGFP-VACV) containing the EGFP gene driven by a synthetic VACV early-late promoter inserted into the *thymidine kinase* (*tk*) locus, and vaccinia virus containing EGFP-tagged versions of the core protein A5 (WR-EGFP-CORE) were generated as previously described ([Mercer and Helenius, 2008](#)). AraC, CHX, and MG132 were purchased from Sigma. UBEI-41 (PYR-41) was purchased from Calbiochem.

Flow Cytometry Analysis and Perturbant Analysis

To analyze temporal viral gene expression, cells were infected with recombinant VACV viruses that express EGFP from the J2R early viral promoter (E-EGFP-VACV) or the F18R late viral promoter (L-EGFP-VACV). Cells were infected at an MOI of 1. For all experiments, cells were harvested at 6 hpi and prepared as previously described ([Mercer and Helenius, 2008](#)). Cells expressing early or late EGFP were gated based on uninfected controls. CHX and AraC served as specific controls for inhibition of early and late gene expression, respectively. Flow cytometry was performed on a BD Bioscience Calibur System. For each sample, 10,000 cells were analyzed. For all experiments, cells were infected with E- or L-EGFP-VACV in the presence of drug at an MOI of 1, unless otherwise indicated.

Viral DNA Uncoating

HeLa cells were infected in the presence of CHX (25 μg/ml), AraC (10 μM), MG132 (25 μM), or UBEI-41 (50 μM). Cells were then infected at an MOI of 10. Four hpi cells were fixed and stained with antisera directed against vaccinia I3L protein (1:500) (a generous gift of Jacomine Krijnse-Locker; University of Heidelberg, Germany) followed by Alexa594 secondary antibody (1:1000) and dra_q5 (1:5000). Images were acquired on a Zeiss LSM 510 confocal microscope at 100X oil immersion objective.

Virion Ubiquitin Immunoblot Analysis

One to five micrograms of band-purified wild-type (WT) MVs were left untreated or were fractionated into membrane and core components as previously described ([Mercer and Traktman, 2003](#)). Samples were separated on SDS-PAGE, transferred to nitrocellulose, and immunoblot analysis was per-

formed for total mono- and polyubiquitination (clone FK2, Enzo Life sciences), k48-linked ubiquitin chains (clone Apu2; Millipore), or K63-linked ubiquitin chains (clone Apu3; Millipore).

siRNA Transfection

For siRNA transfection, 25,000 HeLa ATCC cells were seeded in a 24 well dish 1 day prior to transfection. A 20 nM final concentration of siRNA was used to transfect cells 72 hr prior to infection. siRNAs were purchased from QIAGEN: Cullin1: (1) Hs_CUL1_6; (2) Hs_CUL1_5; (3) Hs_CUL1_3, Cullin3: (1) Hs_CUL3_5; (2) Hs_CUL3_8; (3) Hs_CUL3_10, and Rbx1: (1) Hs_RBX1_6; (2) Hs_RBX1_5; (3) Hs_RBX1_10.

siRNA Depletion Confirmation

Immunoblot analyses to confirm the depletion of target proteins by siRNA were performed on siRNA-treated cells. Antibodies were directed against Cullin1 (1:250; Zymed Laboratories), Skp1 (1:1000; Cell Signaling Technology), or Rbx1 (1:250; Sigma-Aldrich). Cul3 antibody (1:1000) was a generous gift of Prof. M. Peter (Institute of Biochemistry, ETH Zurich).

SUPPLEMENTAL INFORMATION

Supplemental Information includes Extended Experimental Procedures, eight figures, two tables, and a supplemental network visualization algorithm and can be found with this article online at <http://dx.doi.org/10.1016/j.celrep.2012.09.003>.

LICENSING INFORMATION

This is an open-access article distributed under the terms of the Creative Commons Attribution-Noncommercial-No Derivative Works 3.0 Unported License (CC-BY-NC-ND; <http://creativecommons.org/licenses/by-nc-nd/3.0/legaldcode>).

ACKNOWLEDGMENTS

We thank T. Steiger and O. Byrde for data storage and cluster computing, Pauli Rämö for statistical and image analysis, Karin Mench for technical assistance, and Jacomine Krijnse-Locker for anti-I3L. J.M. is supported by an SNF Ambizione (PZ00P3_131988), L.P. by the University of Zurich, SNSF, SystemsX.ch (<http://SystemsX.ch>) RTD project InfectX, and the European Union, C.K.E.B. by the SNF Sinergia CRSII3_125110 and the SystemsX.ch RTD project C-CINA, and A.H. by ETH Zurich, InfectX, and an ERC advanced investigator grant.

Received: July 26, 2012
Revised: August 30, 2012
Accepted: September 7, 2012
Published online: October 18, 2012

WEB RESOURCES

The URLs for data presented herein are as follows:

CellClassifier, <http://www.cellclassifier.ethz.ch>
CellProfiler, <http://www.cellprofiler.org/>
Full set of images and analysis results, <http://www.infectome.org>
STRING database, <http://www.string-db.org>

REFERENCES

Banks, L., Pim, D., and Thomas, M. (2003). Viruses and the 26S proteasome: hacking into destruction. *Trends Biochem. Sci.* 28, 452–459.
Barry, M., van Buuren, N., Bures, K., Mottet, K., Wang, Q., and Teale, A. (2010). Poxvirus exploitation of the ubiquitin-proteasome system. *Viruses* 2, 2356–2380.

- Beard, P.M., Froggatt, G.C., and Smith, G.L. (2006). Vaccinia virus kelch protein A55 is a 64 kDa intracellular factor that affects virus-induced cytopathic effect and the outcome of infection in a murine intradermal model. *J. Gen. Virol.* *87*, 1521–1529.
- Bray, M.A., Fraser, A.N., Hasaka, T.P., and Carpenter, A.E. (2012). Workflow and metrics for image quality control in large-scale high-content screens. *J. Biomol. Screen.* *17*, 266–274.
- Carpenter, A.E., Jones, T.R., Lamprecht, M.R., Clarke, C., Kang, I.H., Friman, O., Guertin, D.A., Chang, J.H., Lindquist, R.A., Moffat, J., et al. (2006). CellProfiler: image analysis software for identifying and quantifying cell phenotypes. *Genome Biol.* *7*, R100.
- Cherry, S. (2009). What have RNAi screens taught us about viral-host interactions? *Curr. Opin. Microbiol.* *12*, 446–452.
- Chiu, W.L., Lin, C.L., Yang, M.H., Tzou, D.L., and Chang, W. (2007). Vaccinia virus 4c (A26L) protein on intracellular mature virus binds to the extracellular cellular matrix laminin. *J. Virol.* *81*, 2149–2157.
- Cho, Y.S., Challa, S., Moquin, D., Genga, R., Ray, T.D., Guildford, M., and Chan, F.K. (2009). Phosphorylation-driven assembly of the RIP1-RIP3 complex regulates programmed necrosis and virus-induced inflammation. *Cell* *137*, 1112–1123.
- Chung, C.S., Chen, C.H., Ho, M.Y., Huang, C.Y., Liao, C.L., and Chang, W. (2006). Vaccinia virus proteome: identification of proteins in vaccinia virus intracellular mature virion particles. *J. Virol.* *80*, 2127–2140.
- Clague, M.J., and Urbé, S. (2010). Ubiquitin: same molecule, different degradation pathways. *Cell* *143*, 682–685.
- Dales, S. (1963). The uptake and development of vaccinia virus in strain L cells followed with labeled viral deoxyribonucleic acid. *J. Cell Biol.* *18*, 51–72.
- Di Giulio, D.B., and Eckburg, P.B. (2004). Human monkeypox: an emerging zoonosis. *Lancet Infect. Dis.* *4*, 15–25.
- Domi, A., and Beaud, G. (2000). The punctate sites of accumulation of vaccinia virus early proteins are precursors of sites of viral DNA synthesis. *J. Gen. Virol.* *81*, 1231–1235.
- Eppstein, D.A., Marsh, Y.V., Schreiber, A.B., Newman, S.R., Todaro, G.J., and Nestor, J.J., Jr. (1985). Epidermal growth factor receptor occupancy inhibits vaccinia virus infection. *Nature* *318*, 663–665.
- Essbauer, S., Meyer, H., Porsch-Ozcürümeç, M., and Pfeffer, M. (2007). Long-lasting stability of vaccinia virus (orthopoxvirus) in food and environmental samples. *Zoonoses Public Health* *54*, 118–124.
- Froggatt, G.C., Smith, G.L., and Beard, P.M. (2007). Vaccinia virus gene F3L encodes an intracellular protein that affects the innate immune response. *J. Gen. Virol.* *88*, 1917–1921.
- Harrison, S.C., Alberts, B., Ehrenfeld, E., Enquist, L., Fineberg, H., McKnight, S.L., Moss, B., O'Donnell, M., Ploegh, H., Schmid, S.L., et al. (2004). Discovery of antivirals against smallpox. *Proc. Natl. Acad. Sci. USA* *101*, 11178–11192.
- Honeychurch, K.M., Yang, G., Jordan, R., and Hruby, D.E. (2007). The vaccinia virus F13L YPPL motif is required for efficient release of extracellular enveloped virus. *J. Virol.* *81*, 7310–7315.
- Huang, C.Y., Lu, T.Y., Bair, C.H., Chang, Y.S., Jwo, J.K., and Chang, W. (2008). A novel cellular protein, VPEF, facilitates vaccinia virus penetration into HeLa cells through fluid phase endocytosis. *J. Virol.* *82*, 7988–7999.
- Huang da, W., Sherman, B.T., and Lempicki, R.A. (2009). Systematic and integrative analysis of large gene lists using DAVID bioinformatics resources. *Nat. Protoc.* *4*, 44–57.
- Ichihashi, Y., Oie, M., and Tsuruhara, T. (1984). Location of DNA-binding proteins and disulfide-linked proteins in vaccinia virus structural elements. *J. Virol.* *50*, 929–938.
- Joklik, W.K. (1964a). The Intracellular Uncoating of Poxvirus DNA. I. The Fate of Radioactively-Labeled Rabbitpox Virus. *J. Mol. Biol.* *8*, 263–276.
- Joklik, W.K. (1964b). The Intracellular Uncoating of Poxvirus DNA. II. The Molecular Basis of the Uncoating Process. *J. Mol. Biol.* *8*, 277–288.
- Kates, J., and Beeson, J. (1970). Ribonucleic acid synthesis in vaccinia virus. I. The mechanism of synthesis and release of RNA in vaccinia cores. *J. Mol. Biol.* *50*, 1–18.
- Komander, D. (2009). The emerging complexity of protein ubiquitination. *Biochem. Soc. Trans.* *37*, 937–953.
- Lablerte, J.P., Weisberg, A.S., and Moss, B. (2011). The membrane fusion step of vaccinia virus entry is cooperatively mediated by multiple viral proteins and host cell components. *PLoS Pathog.* *7*, e1002446.
- Li, Y., Grenklo, S., Higgins, T., and Karlsson, R. (2008). The profilin:actin complex localizes to sites of dynamic actin polymerization at the leading edge of migrating cells and pathogen-induced actin tails. *Eur. J. Cell Biol.* *87*, 893–904.
- Locker, J.K., Kuehn, A., Schleich, S., Rutter, G., Hohenberg, H., Wepf, R., and Griffiths, G. (2000). Entry of the two infectious forms of vaccinia virus at the plasma membrane is signaling-dependent for the IMV but not the EEV. *Mol. Biol. Cell* *11*, 2497–2511.
- MacCallum, F.O., and McDonald, J.R. (1957). Effect of temperatures of up to 45 degrees C on survival of variola virus in human material in relation to laboratory diagnosis. *Bull. World Health Organ.* *16*, 441–443.
- Magee, W.E., and Miller, O.V. (1968). Initiation of vaccinia virus infection in actinomycin D-pretreated cells. *J. Virol.* *2*, 678–685.
- Malkin, A.J., McPherson, A., and Gershon, P.D. (2003). Structure of intracellular mature vaccinia virus visualized by in situ atomic force microscopy. *J. Virol.* *77*, 6332–6340.
- McNulty, S., Bornmann, W., Schriewer, J., Werner, C., Smith, S.K., Olson, V.A., Damon, I.K., Buller, R.M., Heuser, J., and Kalman, D. (2010). Multiple phosphatidylinositol 3-kinases regulate vaccinia virus morphogenesis. *PLoS ONE* *5*, e10884.
- Mercer, J., and Traktman, P. (2003). Investigation of structural and functional motifs within the vaccinia virus A14 phosphoprotein, an essential component of the virion membrane. *J. Virol.* *77*, 8857–8871.
- Mercer, J., and Helenius, A. (2008). Vaccinia virus uses macropinocytosis and apoptotic mimicry to enter host cells. *Science* *320*, 531–535.
- Mercer, J., Knébel, S., Schmidt, F.I., Crouse, J., Burkard, C., and Helenius, A. (2010). Vaccinia virus strains use distinct forms of macropinocytosis for host-cell entry. *Proc. Natl. Acad. Sci. USA* *107*, 9346–9351.
- Mohr, S., Bakal, C., and Perrimon, N. (2010). Genomic screening with RNAi: results and challenges. *Annu. Rev. Biochem.* *79*, 37–64.
- Moser, T.S., Jones, R.G., Thompson, C.B., Coyne, C.B., and Cherry, S. (2010). A kinome RNAi screen identified AMPK as promoting poxvirus entry through the control of actin dynamics. *PLoS Pathog.* *6*, e1000954.
- Moss, B. (1990). Regulation of vaccinia virus transcription. *Annu. Rev. Biochem.* *59*, 661–688.
- Moss, B., Knipe, D.M., and Howley, P.M. (2007). Poxviridae: The viruses and their replication. In *Fields Virology* (Philadelphia: Lippincott-Raven).
- Nerenberg, B.T., Taylor, J., Bartee, E., Gouveia, K., Barry, M., and Früh, K. (2005). The poxviral RING protein p28 is a ubiquitin ligase that targets ubiquitin to viral replication factories. *J. Virol.* *79*, 597–601.
- Pedersen, K., Snijder, E.J., Schleich, S., Roos, N., Griffiths, G., and Locker, J.K. (2000). Characterization of vaccinia virus intracellular cores: implications for viral uncoating and core structure. *J. Virol.* *74*, 3525–3536.
- Petroski, M.D., and Deshaies, R.J. (2005). Function and regulation of cullin-RING ubiquitin ligases. *Nat. Rev. Mol. Cell Biol.* *6*, 9–20.
- Pires de Miranda, M., Reading, P.C., Tschärke, D.C., Murphy, B.J., and Smith, G.L. (2003). The vaccinia virus kelch-like protein C2L affects calcium-independent adhesion to the extracellular matrix and inflammation in a murine intradermal model. *J. Gen. Virol.* *84*, 2459–2471.
- Rämö, P., Sacher, R., Snijder, B., Begemann, B., and Pelkmans, L. (2009). CellClassifier: supervised learning of cellular phenotypes. *Bioinformatics* *25*, 3028–3030.

- Satheshkumar, P.S., Anton, L.C., Sanz, P., and Moss, B. (2009). Inhibition of the ubiquitin-proteasome system prevents vaccinia virus DNA replication and expression of intermediate and late genes. *J. Virol.* *83*, 2469–2479.
- Schmidt, F.I., Bleck, C.K., Helenius, A., and Mercer, J. (2011). Vaccinia extracellular virions enter cells by macropinocytosis and acid-activated membrane rupture. *EMBO J.* *30*, 3647–3661.
- Schmidt, F.I., Bleck, C.K., and Mercer, J. (2012). Poxvirus host cell entry. *Curr. Opin. Virol.* *2*, 20–27.
- Snijder, B., Sacher, R., Rämö, P., Damm, E.M., Liberali, P., and Pelkmans, L. (2009). Population context determines cell-to-cell variability in endocytosis and virus infection. *Nature* *461*, 520–523.
- Snijder, B., Sacher, R., Rämö, P., Liberali, P., Mench, K., Wolfrum, N., Burleigh, L., Scott, C.C., Verheije, M.H., Mercer, J., et al. (2012). Single-cell analysis of population context advances RNAi screening at multiple levels. *Mol. Syst. Biol.* *8*, 579.
- Szklarczyk, D., Franceschini, A., Kuhn, M., Simonovic, M., Roth, A., Minguéz, P., Doerks, T., Stark, M., Muller, J., Bork, P., et al. (2011). The STRING database in 2011: functional interaction networks of proteins, globally integrated and scored. *Nucleic Acids Res.* *39*(Database issue), D561–D568.
- Teale, A., Campbell, S., Van Buuren, N., Magee, W.C., Watmough, K., Couturier, B., Shipclark, R., and Barry, M. (2009). Orthopoxviruses require a functional ubiquitin-proteasome system for productive replication. *J. Virol.* *83*, 2099–2108.
- Townsley, A.C., Weisberg, A.S., Wagenaar, T.R., and Moss, B. (2006). Vaccinia virus entry into cells via a low-pH-dependent endosomal pathway. *J. Virol.* *80*, 8899–8908.
- Villa, N.Y., Barteel, E., Mohamed, M.R., Rahman, M.M., Barrett, J.W., and McFadden, G. (2010). Myxoma and vaccinia viruses exploit different mechanisms to enter and infect human cancer cells. *Virology* *401*, 266–279.
- Welsch, S., Doglio, L., Schleich, S., and Krijnse Locker, J. (2003). The vaccinia virus I3L gene product is localized to a complex endoplasmic reticulum-associated structure that contains the viral parental DNA. *J. Virol.* *77*, 6014–6028.